Jaesool Shim[1]*
Kisoo Yoo[1]*
Prashanta Dutta[2]

[1]School of Mechanical Engineering, Yeungnam University, Gyeongsan, Gyeonsanbukdo, South Korea
[2]School of Mechanical and Materials Engineering, Washington State University, Pullman, WA, USA

Research Article

Steady-state protein focusing in carrier ampholyte based isoelectric focusing: Part I—Analytical solution

The determination of an analytical solution to find the steady-state protein concentration distribution in IEF is very challenging due to the nonlinear coupling between mass and charge conservation equations. In this study, approximate analytical solutions are obtained for steady-state protein distribution in carrier ampholyte based IEF. Similar to the work of Svensson, the final concentration profile for proteins is assumed to be Gaussian, but appropriate expressions are presented in order to obtain the effective electric field and pH gradient in the focused protein band region. Analytical results are found from iterative solutions of a system of coupled algebraic equations using only several iterations for IEF separation of three plasma proteins: albumin, cardiac troponin I, and hemoglobin. The analytical results are compared with numerically predicted results for IEF, showing excellent agreement. Analytically obtained electric field and ionic conductivity distributions show significant deviation from their nominal values, which is essential in finding the protein focusing behavior at isoelectric points. These analytical solutions can be used to determine steady-state protein concentration distribution for experiment design of IEF considering any number of proteins and ampholytes. Moreover, the model presented herein can be used to find the conductivity, electric field, and pH field.

Additional supporting information may be found in the online version of this article at the publisher's web-site

1 Introduction

IEF is a powerful separation technique that is used to concentrate and isolate amphoteric molecules such as proteins, polypeptides, and amino acids in a pH gradient under the influence of an electric field. In IEF, a pH difference is created between an anode and a cathode by applying an electric current to a system of electrolytes. In the presence of the pH gradient, proteins and other ampholytic molecules (such as ampholytes) are moved in the separation channel due to their electrophoretic mobility until they reach the pH location of zero net charge, which is known as the pI. Thus, a mixture of proteins can be separated in a separation chamber based on their isoelectric points.

Williams and Waterman [1] were the first to clearly present the principle of IEF, although the first known case of separation by electrolysis goes back more than a century. In their separation work, 14 compartments separated by membranes were used to create a steady pH distribution between the anode and cathode. The pH distribution obtained in [1] was a staircase with a constant pH in each compartment and a sharp pH change at the separating membranes. Later, Kolin [2, 3] demonstrated high-resolution separation of proteins in minutes using a smooth pH profile in the separation column. The invention of carrier ampholytes by Vesterberg [4], a mixture of synthetic chemicals with an appreciable conductance and buffering capability, has revolutionized the application of IEF in analytical and preparative scale separations.

Although IEF is widely used in the purification and separation of proteins, the theoretical study of IEF is very challenging due to nonlinear interactions between the electric field and charges of the chemical components used in the buffering electrolyte and target proteins. In 1961, Svensson [5] provided a mathematical description for the behavior of ampholytes in a natural pH gradient, which is the

Correspondence: Professor Prashanta Dutta, FASME, School of Mechanical and Materials Engineering, Washington State University, Pullman, WA 99164, USA
E-mail: prashanta@wsu.edu
Fax: +1-509-335-4662

*These authors contributed equally to this work.

Colour Online: See the article online to view Figs. 1–3 in colour.

starting point for most theoretical analysis in this field. Subsequently, the buffering capacity and the conductivity of carrier ampholytes have been theoretically described and compared with measurements for some simple systems [6, 7]. Through these classical works, Svensson concluded that the isoelectric point of a good ampholyte should be very close to its pK values. Svensson also proposed an analytical solution for ampholyte concentration with a Gaussian distribution at its isoelectric point by considering a nominal pH gradient and a constant electric field. Gelsema and De Ligny [8] analyzed the non-Gaussian concentration distribution of ampholytes in IEF by considering changes in conductivity with respect to pH. Slais [9] analyzed the steady-state behavior of carrier ampholytes in moving pH gradients, and applied this model to show the transition between ITP and IEF. In 1998, Stoyanov and Righetti [10] presented an analytical model for the steady-state concentration distribution of ampholytes in IEF in a linear immobilized pH gradient. Frumin et al. [11] presented a simple analytical formulation to aid in the understanding of the transient behavior of ampholytes in IEF assuming a Gaussian initial concentration profile and a linear migration velocity for the ampholyte. However, in reality, the initial profile of ampholyte is not Gaussian (rather, it is uniform), and the actual velocity of the IEF is not linear.

While considerable progress has been made in understanding the behavior of ampholytes in IEF, no theoretical studies have been reported in the literature on the focusing mechanism of proteins in IEF. Unlike carrier ampholytes, a mathematical description of proteins requires many more pKs, which affects the mean charge and other electromigration properties in the separation channel. In 1983, Bier et al. [12] introduced a unified mathematical model for transient electrophoresis, and presented simulation results for ITP and artificial pH-based IEF. Their mathematical model has been expanded to study protein dynamics in carrier ampholyte based IEF using different numerical models [13–17].

Although numerical models are powerful to elucidate the transient dynamics of proteins and carrier ampholytes during IEF, their application is somewhat limited for general use. Most of the high-performance computer codes [18] are either proprietary or difficult to implement without a significant computing background. Although a number of commercial software packages provide solvers for IEF with a limited number of ampholytes, often they fail to provide converged results for realistic problems. Thus, an analytical solution for protein focusing in carrier ampholyte based IEF will be of great value for IEF experiment design.

In this study, we developed analytical solutions to find protein and ampholyte concentration distributions at the steady state in a carrier ampholyte based IEF. As in other analytical works, the present work is based on the Gaussian concentration distribution for all amphoteric components including proteins at their steady states. However, unlike other works, we did not use a nominal electric field or pH gradient to compute the concentration distribution of proteins. Necessary modifications are made in the pH gradient and electric field distributions in order to obtain the protein

concentration distribution and peak height, which are in good agreement with results presented by high-resolution computer models [18] for an identical system.

2 Theoretical analysis

Detailed mathematical models for carrier ampholyte based IEF are presented in our earlier publication [15] and in other reports [12, 19, 20]. Thus, the full mathematical model is not presented here. Readers can consult the aforementioned classical studies for details on mass and charge conservation equations. In this section, we describe our analysis for the concentration distribution from 1D mass and charge conservation equations for amphoteric components. The approximation and assumptions used in this study are as follows.

(1) At the steady state, the concentration distributions for both proteins and ampholytes are Gaussian.
(2) Both proteins and ampholytes formed very narrow bandwidth peaks at the steady state.
(3) The pH profile is linear along the separation channel.
(4) The hydrogen ion concentration distribution remains same regardless of the existence of proteins.
(5) For an applied electric potential difference along the separation channel, the current densities remain same for IEF systems with and without proteins.
(6) The steady-state ampholyte concentration profile does not change regardless of the existence of protein(s) in the separation channel.
(7) The electric field and pH gradient remain constant within the focused protein band regions.

2.1 Steady-state concentration profile

For IEF in a straight microchannel or capillary as shown in Fig. 1A, the mass conservation equation can be expressed as

$$\frac{\partial C_i}{\partial t} + \frac{dJ_i}{dx} = 0, \tag{1}$$

where C_i is the concentration of amphoteric components (such as proteins and ampholytes) distributed along the separation axis x and J_i is the flux of the amphoteric compounds due to an electric field (E_x). In the absence of pressure-driven or electroosmotic bulk flow, the flux term can be defined as

$$J_i = \langle z_i \rangle \, \omega_i \, E_x(x) \, C_i - D_i \frac{dC_i}{dx}, \tag{2}$$

where ω_i and D_i are the absolute mobility and diffusion coefficients of the ith components, respectively. The effective valence of the ith component can be defined as

$$\langle z_i \rangle = \frac{\sum_{j=1}^{M_i+1} z_{ij} \, S_{ij}}{C_i}, \tag{3}$$

where S_{ij} and z_{ij} are the concentration and valence, respectively, of the jth species within an ith component with M_i dissociable groups.
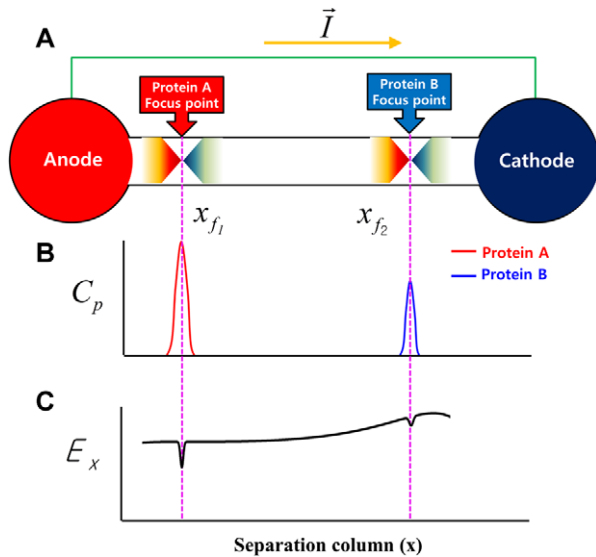
Figure 1. (A) Schematic of IEF in a straight microchannel. A constant current density is applied in order to separate two different proteins in a carrier ampholyte based IEF. (B) At the steady state, proteins are focused at their isoelectric points (pIs). (C) Schematic of local electric field distribution along the separation channel at the steady state.

At the steady state and for no-flux boundary conditions at the anolyte and catholyte reservoirs, Eqs. (1) and (2) can be simplified to $J_i = 0$, which can be rewritten as

$$\frac{dC_i}{C_i} = \frac{\omega_i E_x(x)}{D_i} \langle z_i \rangle \, dx. \tag{4}$$

For an amphoteric component, the effective valence, $\langle z_i \rangle$, is a function of column axis x. For ampholytes, the effective valence can be found from the pK values, while for proteins, it can readily be found from titration curve of the protein. Thus, if the functional relationship is known, the value of the effective valence at any location in close proximity to a pI ($x = x_{f,i}$) can be obtained from a Taylor series as

$$\langle z_i \rangle = (x - x_{f_i}) \left. \frac{d\langle z_i(x) \rangle}{dx} \right|_{x=x_{f_i}}$$

$$+ \frac{1}{2}(x - x_{f_i})^2 \left. \frac{d^2 \langle z_i(x) \rangle}{dx^2} \right|_{x=x_{f_i}} + \cdots \tag{5}$$

If an amphoteric component focuses very close to its isoelectric location, the value of $(x - x_f)$ can be considered very small at steady state, and the higher-order terms in the series of effective valence diminish. Under this narrow bandwidth assumption, Eq. (4) can be rewritten as

$$\frac{dC_i}{C_i} = \left(\frac{\omega_i}{D_i}(x - x_{f_i}) \left. \frac{d\langle z_i(x) \rangle}{dpH} \right|_{x=x_{f_i}} \right) \left(\left. \frac{dpH}{dx} \right|_{x=x_{f_i}} \right) (E_x) \, dx. \tag{6}$$

Next, we assume that the electric field and the pH gradient remain constant within the focused band region. These assumptions are much more stringent and might seem arbi-

trary, but they are needed to obtain an approximate analytical solution for concentration distribution. Under the aforementioned assumptions, Eq. (6) can be rewritten as

$$\frac{dC_i}{C_i} = \left(\frac{\omega_i}{D_i}(x - x_{f_i}) \left. \frac{d\langle z_i(x) \rangle}{dpH} \right|_{pH=PI} \right) \left(\overline{\frac{dpH}{dx}} \right) (\bar{E}_x) \, dx. \tag{7}$$

Here the bar is used to indicate the constant value within the focused band region. By integrating Eq. (7), we can find an expression for concentration distribution as follows:

$$C_i = B \exp \left(\frac{\omega_i}{2D_i}(x - x_{f_i})^2 \left. \frac{d\langle z_i(x) \rangle}{dpH} \right|_{pH=PI} \right) \left(\overline{\frac{dpH}{dx}} \right) (\bar{E}_x)$$

$$= B \, e^{-\frac{1}{2}\left(\frac{x - x_{f_i}}{\sigma_i}\right)^2}, \tag{8}$$

where B is an integration constant. Equation (8) provides a Gaussian concentration distribution at its focal points x_{f_i} with inflection points at the standard deviation (σ_i) as follows:

$$\sigma_i = \sqrt{-\frac{D_i}{\omega_i \left. \frac{d\langle z_i \rangle}{dpH} \right|_{pH=pI} \left(\overline{\frac{dpH}{dx}} \right) (\bar{E}_x)}}. \tag{9}$$

If we assume a uniform initial concentration distribution ($C_{i,0}$) along the channel, the integration constant B can be obtained by integrating the concentration distribution $C_i(x)$ along the separation column and equating that with the total mass of the components:

$$B = \frac{L \cdot C_{i,0}}{\sqrt{2\pi}\sigma_i}. \tag{10}$$

Substitution of Eq. (10) into Eq. (8) yields a steady-state concentration distribution along the channel:

$$C_i = \frac{L \cdot C_{i,0}}{\sqrt{2\pi}\sigma_i} e^{-\frac{1}{2}\left(\frac{x - x_{f_i}}{\sigma_i}\right)^2}. \tag{11}$$

We note that the concentration distribution can only be obtained if the standard deviation of the focused band is known. As presented in Eq. (9), the standard deviation of a focused band depends on an effective pH gradient, $\overline{\frac{dpH}{dx}}$, and an effective electric field, $\bar{E}_x$, for the protein band, which are not known. One option is to compute them based on the nominal pH gradient and electric field. However, a recent numerical study shows that the electric field drops significantly at the location of focused proteins [21], and the deviation is very significant from the nominal electric field. Thus, it would be a mistake to use the nominal electric field for the determination of protein concentration. The electric field variation is even quite severe in the broad pH range IEF. In this study, we considered an alternate technique to find the concentration distribution, especially for focused proteins.

2.2 Relation between current density and electric field at the steady state

In the absence of a bulk fluid flow, the current density I in an electrolyte system can be defined as

$$I = F \sum_{i=1}^{\Lambda} \left(-D_i \nabla \left(\langle z_i \rangle C_i \right) + \langle z_i^2 \rangle \omega_i E_x(x) C_i \right), \tag{12}$$

where $J_{ij} = -D_{ij} S_{ij} + z_{ij} \omega_{ij} E_x(x) S_{ij}$ and $\langle z_i^2 \rangle = \sum_{j=1}^{M_i+1} z_{ij}^2 S_{ij}/C_i$. D_{ij} and ω_{ij} are the diffusion coefficient and absolute mobility of the jth species within the ith component, respectively; F is the Faraday constant; and Λ is the total number of components in the system. At the steady state, the current density can be simplified as follows:

$$I = F \langle z_i^2 \rangle \omega_i E_x(x) C_i = \kappa_i(x) \cdot E_x(x) = const, \tag{13}$$

where the ionic conductivity is defined as

$$\kappa_i = F \langle z_i^2 \rangle \omega_i C_i. \tag{14}$$

Thus, the local electric field along the separation channel can be obtained from

$$E_x(x) = \frac{I}{\kappa(x)}. \tag{15}$$

Since the current density remains constant, integration of Eq. (15) along the separation axis gives a relationship between the potential difference and the ionic conductivity as follows:

$$I = \frac{\int_o^L E_x(x)\,dx}{\int_o^L \frac{1}{\kappa(x)}\,dx} = \frac{\int_o^L \left(\frac{dV}{dx} \right) dx}{\int_o^L \frac{1}{\kappa(x)}\,dx} = \frac{V}{\int_o^L \frac{1}{\kappa(x)}\,dx}, \tag{16}$$

where V is the potential at the anode, while the cathode is grounded.

2.3 Electric field correction in the presence of proteins

In a carrier ampholyte based IEF, the local conductivity increases sharply at the location of a protein isoelectric point, which results in a decrease in the local electric field [21]. To evaluate the local electric field at the location of a protein isoelectric point, we considered two separate IEF systems. The first system is comprised of ampholytes only, and the second system has both carrier ampholytes and proteins. We assume that the conductivity distribution along the channel is known for the first case.

The current density for the first and second systems can be expressed as

$$I_{\text{system1}} = \kappa(x)_a \cdot E_x(x)_a, \tag{17a}$$

$$I_{\text{system2}} = (\kappa(x)_{a+p}) \cdot \left(E_x(x)_{a+p} \right), \tag{17b}$$

where $(E_x(x))_a$ is the local electric field for the first system (ampholytes only) at the steady state, which can be obtained from the local conductivity information at the steady

state. The conductivity of the second system, as presented in Eq. (17b), can be decomposed into two components:

$$\kappa(x)_{a+p} = \kappa(x)_a^* + \kappa(x)_p, \tag{18}$$

where subscripts "a" and "p" are used to denote ampholytes and proteins and $\kappa(x)_a^*$ represents the conductivity of ampholytes in the presence of proteins. We assume that the current density is same for both cases at the steady state. This assumption is particularly valid for a 1D system since focused proteins only affect the conductivity and electric field distribution at their pIs. In other words, the local electric field and conductivity do not change in regions away from the focused protein bands. Based on the aforementioned assumption, the local current density can be expressed as

$$(\kappa(x)_a) \cdot (E_x(x)_a) \cong (\kappa(x)_a^* + \kappa(x)_p) \cdot \left(E_x(x)_{a+p} \right). \tag{19}$$

In the proximity of a protein isoelectric point, although the concentration of the ampholytes is reduced slightly as compared to that of ampholytes with no protein, the conductivity change can be considered negligible. Thus,

$$\kappa(x)_a^* \cong \kappa(x)_a. \tag{20}$$

Using Eqs. (19) and (20), a relationship between the electric field with and without proteins can be defined as

$$E_x(x)_{a+p} = \frac{\kappa(x)_a}{\kappa(x)_a + \kappa(x)_p} \cdot (E_x(x)_a) = f_e(x) \cdot (E_x(x)_a), \tag{21}$$

where a correction factor in the electric field can be given by

$$f_e(x) = \frac{\kappa(x)_a}{\kappa(x)_a + \kappa(x)_p}. \tag{22}$$

Equation (22) indicates that the electric field in the protein region decreases with an increase in the conductivity of proteins. A careful examination of Eq. (22) reveals that the correction factor for the electric field follows the same Gaussian distribution of protein concentration. The minima of the correction factor profile will occur at the isoelectric points of proteins, and the local electric field correction will approach unity at other locations. Thus, the minima of $f_e(x)$ can be obtained as follows:

$$f_{e,p,\min} = \frac{\kappa_a}{\kappa_a + F \left(\langle z_p^2 \rangle \omega_p C_p \right)_{pH=pI}}, \tag{23}$$

where $C_p|_{pH=pI}$ is the concentration of a protein at its pI point. If the electric field correction factor is known at the location of the protein isoelectric point, Eq. (21) can be written as

$$E_x(x)_{a+p} = \left(1 - \left(1 - f_{e,p,\min} \right) \cdot e^{-\frac{1}{2} \left(\frac{x - x_{f_p}}{\sigma_p} \right)^2} \right) E_x(x)_a. \tag{24}$$

2.4 Correction of pH gradient

It is well known that the concentration of hydronium can be obtained from the electroneutrality equation. We now

reconsider the two previously described IEF systems. The electroneutrality equation for a system without proteins is

$$\sum \left(\langle z_a \rangle \, C_a \right) + C_H - \frac{K_w}{C_H} = 0. \tag{25}$$

Similarly, the electroneutrality equation for a system with proteins can be expressed as

$$\sum \left(\langle z_a \rangle \, C_a^* \right) + \sum \left(\langle z_p \rangle \, C_p \right) + C_H^* - \frac{K_w}{C_H^*} = 0, \tag{26}$$

where asterisks are used to indicate the presence of protein in the system. If we assume a linear pH profile for both cases, the concentrations of hydronium are almost same ($C_H \approx C_H^*$) in all separation regions. Thus, Eqs. (25) and (26) can be rewritten as

$$\left(\sum \langle z_a \rangle \, C_a^* \right) = - \sum \left(\langle z_p \rangle \, C_p \right) + \left(\sum \langle z_a \rangle \, C_a \right). \tag{27}$$

The derivative of Eq. (27) with respect to x yields

$$\frac{d \left(\sum \langle z_a \rangle \, C_a^* \right)}{dx} = - \frac{d \left(\sum \left(\langle z_p \rangle \, C_p \right) \right)}{dx} + \frac{d \left(\sum \langle z_a \rangle \, C_a \right)}{dx}. \tag{28}$$

The rearrangement of derivatives gives

$$\sum \left(\frac{d \langle z_a \rangle}{d(pH)^*} \frac{d(pH)^*}{dx} (C_a)^* \right) + \sum \left(\frac{d(C_a)^*}{dx} \langle z_a \rangle \right)$$
$$= - \sum \frac{d \langle z_p \rangle}{d(pH)^*} \frac{d(pH)^*}{dx} (C_p) - \sum \frac{d (C_p)}{dx} \langle z_p \rangle$$
$$+ \sum \left(\frac{d \langle z_a \rangle}{d (pH)} \frac{d (pH)}{dx} (C_a) \right) + \sum \left(\frac{d(C_a)}{dx} \langle z_a \rangle \right). \tag{29}$$

If we assume that the concentrations of ampholyte do not change significantly between two systems, one can come up with following expressions

$$\sum \left(\frac{d(C_a)^*}{dx} \langle z_a \rangle \right) \approx \sum \left(\frac{d(C_a)}{dx} \langle z_a \rangle \right), \tag{30}$$

$$\sum \left(\frac{d \langle z_a \rangle}{d(pH)^*} (C_a)^* \right) \approx \sum \left(\frac{d \langle z_a \rangle}{d (pH)} (C_a) \right). \tag{31}$$

Using Eqs. (29) to (31), we obtain the pH gradient relationship with and without proteins as follows:

$$\left(\frac{d(pH)^*}{dx} \right) = \frac{\left(\sum \frac{d \langle z_a \rangle}{d(pH)} (C_a) \right)}{\left(\sum \frac{d \langle z_a \rangle}{d(pH)} (C_a) \right) + \sum \frac{d \langle z_p \rangle}{d(pH)^*} C_p(x)} \left(\frac{d (pH)}{dx} \right)$$
$$- \frac{\sum \frac{d(C_p)}{dx} \langle z_p \rangle}{\left(\sum \frac{d \langle z_a \rangle}{d(pH)} (C_a) \right) + \sum \frac{d \langle z_p \rangle}{d(pH)^*} C_p(x)}, \tag{32}$$

where $\frac{d(pH)^*}{dx}$ and $\frac{d(pH)}{dx}$ are the pH gradient in the system with and without the presence of proteins, respectively.

2.5 Concentration of ampholytes at the steady state

In order to calculate a pH gradient correction, concentrations of ampholytes are needed at the steady state. Like proteins, steady-state concentration profiles for ampholytes can

be modeled using a Gaussian profile. Thus, for the concentration of ampholytes, Eq. (11) can be written as

$$C_a = \frac{L \cdot C_{a,t=0}}{\sqrt{2\pi} \, \sigma_a} e^{- \frac{1}{2} \left(\frac{x - x_{fa}}{\sigma_a} \right)^2}. \tag{33}$$

For ampholytes, Svensson suggested that the location of the inflection point can be found with a nominal pH gradient and local electric field at their isoelectric points (x_{fa}) as [5]

$$\sigma_a = \sqrt{ \left(\frac{D_a}{\omega_a} \right) \left(\frac{-1}{\left. \frac{d \langle z_a \rangle}{d pH} \right|_{pH = pI,a} \frac{\Delta pH}{L} E_x(x = x_{fa})} \right) }. \tag{34}$$

To calculate the ampholyte concentration distribution, we must know the net charge distribution for ampholytes along the channel. Unlike protein, titration curves are not available for ampholytes. However, this relation can be established from the pK values of ampholytes. For a biprotic ampholyte with three charge states ($K_{a,1}$ and $K_{a,2}$), the effective valence of ampholytes can be expressed as

$$\langle z_a \rangle = \frac{C_H^2 - K_{a,1} K_{a,2}}{C_H^2 + K_{a,1} C_H + K_{a,1} K_{a,2}}, \tag{35}$$

where $K_{a,1} = 10^{-pI_a + \frac{\Delta pK}{2}}$ and $K_{a,2} = 10^{-pI_a - \frac{\Delta pK}{2}}$. If we take the derivative of Eq. (35) with respect to C_H and use pH $= -\log_{10} C_H$, then

$$\frac{d \langle z_a \rangle}{dpH} = -ln(10) \frac{K_{a,1} C_H \left(C_H^2 + 4 K_{a,2} C_H + K_{a,1} K_{a,2} \right)}{\left(C_H^2 + K_{a,1} C_H + K_{a,1} K_{i,2} \right)^2}. \tag{36}$$

At ampholyte pI points, the hydronium concentration can be expressed as

$$C_H = 10^{-pI_a}. \tag{37}$$

Using Eqs. (35) to (37), we obtain

$$\left. \frac{d \langle z_a \rangle}{dpH} \right|_{pH = pI,a} = - \frac{2 \ln(10)}{2 + 10^{\Delta pK/2}}. \tag{38}$$

2.6 Effective electric field and pH gradient for proteins

To find the protein concentration distribution using Eq. (11), we must know the effective electric field ($\bar{E}_x$) and pH gradient ($\frac{dpH}{dx}$). In this section, we describe a method to find the effective electric field and pH gradient from the expressions of the local electric field and pH gradients. The effective electric field within the focused protein band can be obtained as

$$\bar{E}_x = \frac{1}{2\alpha\sigma} \int_{-\alpha\sigma}^{\alpha\sigma} f_e(x) \cdot (E_x(x))_a dx \tag{39}$$

where α is a constant. In [6], it was suggested that two well-resolved Gaussian peaks should be separated by 3σ. Thus, in the present study, we set $\alpha = 1.5$, though other values of α are also investigated (See Supporting Information

Table 1). Based on aforementioned assumption, the electric field equation can be rewritten as

$$\bar{E}_x = 1 - 0.7295 \left(1 - \left(f_e(x)\right)_{\min}\right) \left(E_x(x)\right)_{amp}. \tag{40}$$

The local pH gradient profile described by Eq. (32) is quite cumbersome. Thus, we attempt to make some simplifications for an approximate analytical work. At the isoelectric points of proteins, $\frac{d(C_p)}{dx}\big|_{x=x_{f_p}} = 0$. Hence, Eq. (32) can be reduced at the protein isoelectric point as follows:

$$\left(\frac{d(pH)^*}{dx}\right)\Bigg|_{x=x_{f_p}}$$

$$= \frac{\left(\sum \frac{d\langle z_a\rangle}{d(pH)}(C_a)\right)\Big|_{x=x_{f_a}}}{\left(\sum \frac{d\langle z_a\rangle}{d(pH)}(C_a)\right)\Big|_{x=x_{f_a}} + \sum \frac{d\langle z_p\rangle}{d(pH)^*} C_p(x)\Big|_{x=x_{f_p}}}$$

$$\times \left(\frac{d(pH)}{dx}\right)\Bigg|_{x=x_{f_p}}. \tag{41}$$

Equation (41) can also be rewritten as

$$\left(\frac{d(pH)^*}{dx}\right)\Bigg|_{x=x_{f_p}} = f_{pH,p,\min}\left(\frac{d(pH)}{dx}\right)\Bigg|_{x=x_{f_p}}, \tag{42}$$

where

$$f_{pH,p,\min} = \frac{\left(\sum \frac{d\langle z_a\rangle}{d(pH)}(C_a)\right)\Big|_{x=x_{f_a}}}{\left(\sum \frac{d\langle z_a\rangle}{d(pH)}(C_a)\right)\Big|_{x=x_{f_a}} + \sum \frac{d\langle z_p\rangle}{d(pH)^*} C_p(x)\Big|_{x=x_{f_p}}}. \tag{43}$$

Thus, one can present the local pH gradient with a Gaussian distribution

$$\frac{d(pH)^*}{dx} = \left(1 - \left(1 - f_{pH,p,\min}\right) e^{-\frac{1}{2}\left(\frac{x-x_{f_p}}{\sigma_p}\right)^2}\right) \frac{\Delta pH}{L}. \tag{44}$$

Like the effective electric field, the effective pH gradient can be obtained as

$$\overline{\frac{dpH}{dx}} = 1 - 0.7295 \left(1 - f_{pH,p,\min}\right) \frac{\Delta pH}{L}. \tag{45}$$

Therefore, using Eqs. (40) and (45), the location of inflection points for proteins can be given as

2.7 Focused concentration of proteins at the steady state

At the steady state, the local concentration distribution of proteins can be obtained from Eq. (11) as follows:

$$C_p = \frac{L \cdot C_{p,\,t=0}}{\sqrt{2\pi}\sigma_p} e^{-\frac{1}{2}\left(\frac{x-x_{f_p}}{\sigma_p}\right)^2} \tag{47}$$

with a maximum concentration at the pI point:

$$\left(C_p\right)_{x=pI} = C_p^{\max} = \frac{L \cdot C_{p,t=0}}{\sqrt{2\pi}\sigma_p}. \tag{48}$$

Although an approximate analytical solution is presented in Eq. (47) for protein concentration, it is not straightforward to compute protein concentration for a particular protein. Equations (23), (43), (46), (33), and (47) must be solved simultaneously to find $f_{e,p,\min}$, $f_{pH,p,\min}$, σ_p, C_a, and C_p. There are five algebraic equations for aforementioned five variables, and these variables can be determined using an iterative computer algorithm. An MATLAB-based computer program is provided in the Supporting Information for that.

3 Discussion

Analytical expressions are very useful for experiment design and numerical validation. In this section, an IEF case study is presented using the analytical model developed in Section 2. The problem geometry considered in this case is shown in Fig. 1. Fifty biprotic ampholytes ($\Delta pK = 3$) are used to generate a pH profile between 6 and 9 within a 2-cm-long channel. The absolute mobility of the ampholytes is 3×10^{-8} m^2/(Vs), and the diffusion coefficients are obtained from the Nernst–Einstein equation. The initial concentration of each ampholyte is 0.45 mM.

Three different proteins—albumin, cTnI, and hemoglobin—were separated by using an electric current between the anolyte and catholyte reservoir. The titration curves for these proteins are shown in Fig. 2. The charge data were obtained from the protein data bank (http://www.uniprot.org). The physicochemical properties of these proteins and their initial concentrations are shown in Table 1. Here, the mean square charge ($\langle z_i^2\rangle$) for a protein is calculated from [18]

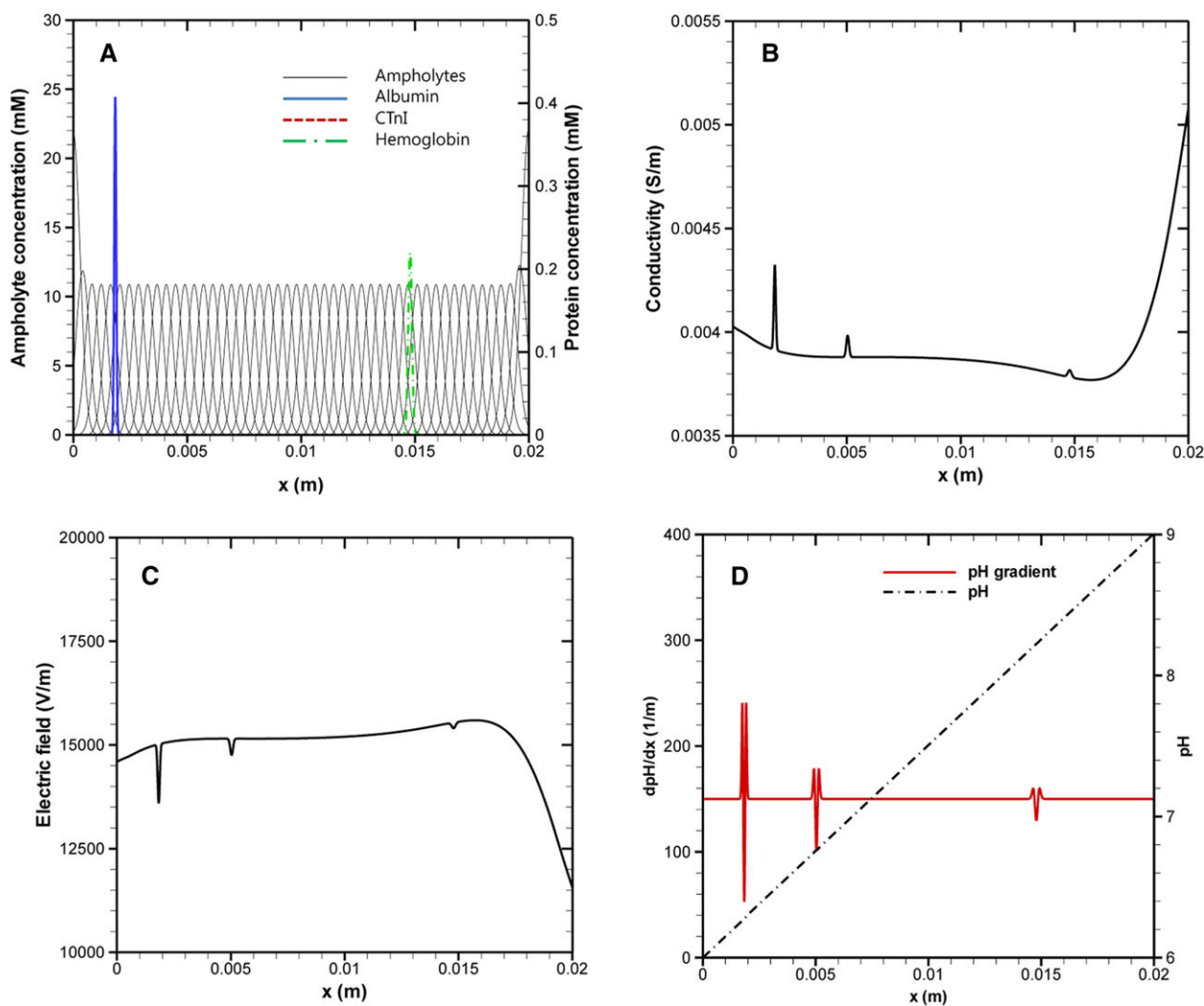$$\langle z_i^2\rangle = \left[f_i(pH)\right]^2 - \frac{1}{\ln(10)} \frac{df_i(pH)}{dpH}, \tag{49}$$

$$\sigma_p = \sqrt{\left(\frac{RT}{F}\right)\left(\frac{-1}{\frac{d\langle z_i\rangle}{dpH}\big|_p \frac{\Delta pH}{L} \left(\left(E_x\right)_a\right)\left(1 - \chi\left(1 - f_{e,p,\min}\right)\right)\left(1 - \chi\left(1 - f_{pH,p,\min}\right)\right)}\right)}, \tag{46}$$

where $\chi = 0.7295$ for $\alpha = 1.5$, and $\frac{D_p}{\omega_p} = \frac{RT}{F}$.

where $f_i(pH)$ is a titration function developed by polynomial fitting. As mentioned in Section 2.6, the concentration of
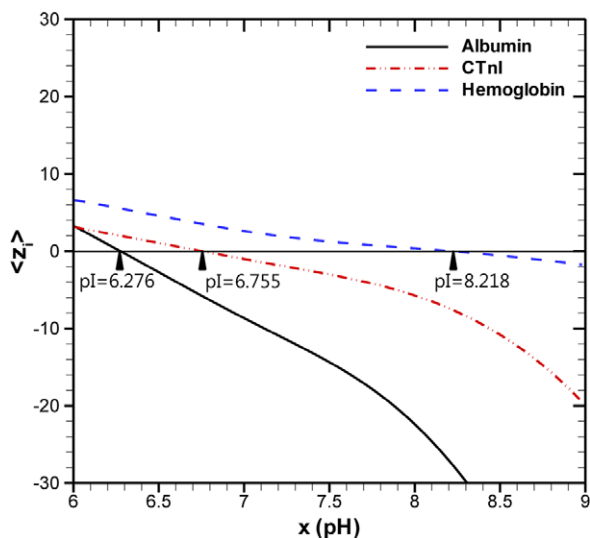
Figure 2. Titration curves of three proteins used for IEF in a microchannel.

Table 1. Physicochemical properties of proteins used in this study

	Albumin	cTnI	Hemoglobin	Unit
pI	6.276	6.755	8.218	—
$\frac{d\langle z_p \rangle}{dpH}\vert_{pI_p}$	−12	−4.174	−1.854	—
$\langle z_p^2 \rangle \vert_{pI_p}$	5.2115	1.8127	0.8052	—
ω_p	2.00×10^{-9}	2.00×10^{-9}	2.00×10^{-9}	m^2/(Vs)
$C_{p,t=0}$	0.00225	0.00225	0.00225	mM

proteins can be obtained iteratively from the solution of a number of algebraic equations.

Determination of protein concentration requires the information of the ampholyte concentration. In this study, we use ampholyte conductivity distribution as input data since they are available from the ampholyte manufacturer. Based on the steady-state ampholyte conductivity ($\kappa(x)_a$) and an applied electric current density (I), we can determine the electric

Figure 3. Steady-state IEF results in a straight microchannel for an applied current density of 58.8 A/m^2. (A) Protein and ampholyte concentration, (B) conductivity, (C) electric field distribution, and (d) pH gradient as well as pH profile along the microchannel.

Table 2. Comparison of analytical results with corresponding numerical values for peak concentration

	Albumin (mM)	cTnl (mM)	Hemoglobin (mM)
Numerical	0.401	0.307	0.220
Analytical	0.407	0.298	0.220
Percentage difference	1.49%	2.93%	0%

field distribution ($E_x(x)_a$) from Eq. (17a). Then, Eq. (33) can be used to find the ampholyte concentration, where the standard deviation for the ampholyte band can be found from Eq. (34) using the nominal pH gradient, slope of the ampholyte charge Eq. (38), and local electric field ($E_x(x)_a$). Finally, the protein concentration can be calculated by using Eq. (47), wherein the standard deviation of the focused protein band can be determined from Eq. (46) using the values of $f_{e,p,min}$ and $f_{pH,p,min}$ given by Eqs. (23) and (43), respectively.

Figure 3(A) shows the steady-state protein concentration distribution in a microchannel for an applied current density of 58.8 A/m^2. Although the initial concentrations were the same for all three proteins, the peak height of albumin is the highest, whereas the peak height of hemoglobin is the lowest at the steady state. This occurs because the slope of the titration curve is the steepest for albumin at its pI point, and the slope is much flatter for hemoglobin. Results obtained from the approximate analytical solutions are in good agreement with the numerical results, wherein a finite volume based numerical technique [15] is used to generate the protein concentration distribution for a similar system. Table 2 shows a comparison between the analytical and numerical results for all three proteins. The corresponding ionic conductivity, electric field, and pH distribution are also shown in Fig. 3B–D. The conductivity and electric field distributions are inline with reports in the literature [21]. The conductivity (electric field) rise (drop) is the highest at the location of the albumin pI because of a much higher value of the square of the mean charge ($\langle z_i^2 \rangle$) for albumin compared to others (see Table 1). Further validation, as well as limitation of the analytical model, is presented in a companion paper [22].

4 References

[1] William, R. R., Waterman, R. E., *Proc. Soc. Exp. Biol. Med.* 1929, *27*, 56–61.

[2] Kolin, A., *J. Chem. Phys.* 1954, *22*, 1628–1629.

[3] Kolin, A., *Proc. Natl. Acad. Sci. USA* 1955, *41*, 101–110.

[4] Vesterberg, O., *Acta Chem. Scand.* 1969, *23*, 2653–2666.

[5] Svensson, H., *Acta Chem. Scand.* 1961, *15*, 325–341.

[6] Rible, H., *Ann. N. Y. Acad. Sci.* 1973, *209*, 11–22.

[7] Svensson, H., *Acta Chem. Scand.* 1962, *16*, 456–466.

[8] Gelsema, W. J., De Ligny, C. L., *J. Chromatogr.* 1979, *178*, 550–554.

[9] Slais, K., *J. Microcolumn Sep.* 1993, *5*, 469–479.

[10] Stoyanov, A. V., Righetti, P. G., *Electrophoresis* 1998, *19*, 1596–1600.

[11] Frumin, L. L., Zilberstein, G. V., Peltek, S. E., *J. Biochem. Biophys. Methods* 2000, *45*, 205–209.

[12] Bier, M., Palusinski, O. A., Mosher, R. A., Saville, D. A., *Science* 1983, *219*, 1281–1287.

[13] Shimao, K., *Electrophoresis* 1987, *8*, 14–19.

[14] Mosher, R. A., Thormann, W., *Electrophoresis* 2002, *23*, 1803–1814.

[15] Shim, J., Dutta, P., Ivory, C. F., *Electrophoresis* 2007, *28*, 572–586.

[16] Shim, J., Dutta, P., Ivory, C. F., *J. Nanosci. Nanotechnol.* 2008, *8*, 3719–3728.

[17] Shim, J., Dutta, P., Ivory, C. F., *Electrophoresis* 2008, *29*, 1026–1035.

[18] Yoo, K., Shim, J., Liu, J., Dutta, P., *Electrophoresis* 2014, *35*, 638–645.

[19] Palusinski, O. A., Bier, M., Saville, D. A., *Biophys. Chem.* 1981, *14*, 389–397.

[20] Saville, D. A., Palusinski, O. A., *AIChE J.* 1986, *32*, 207–214.

[21] Yoo, K., Shim, J., Dutta, P., *Biomicrofluidics* 2014, *8*, 064125.

[22] Shim, J., Yoo, K., Dutta, P., *Electrophoresis* 2017.